Appendix 1

SUPPLEMENTARY INFORMATION FOR CHAPTER 2: EVALUATING MOLECULAR COBALT COMPLEXES FOR THE CONVERSION OF N_2 TO NH_3

Reproduced in part with permission from:

Del Castillo, T. J.; Thompson, N. B.; Suess, D. L.; Ung, G.; Peters, J. C.; *Inorg. Chem.*, **2015**, 54, 9256-9262. **DOI:** 10.1021/acs.inorgchem.5b00645

A1.1 General considerations:

All manipulations were carried out using standard Schlenk or glovebox techniques under an N_2 atmosphere. Solvents were deoxygenated and dried by thoroughly sparging with N_2 followed by passage through an activated alumina column in a solvent purification system by SG Water, USA LLC. Nonhalogenated solvents were tested with sodium benzophenone ketyl in tetrahydrofuran in order to confirm the absence of oxygen and water. Deuterated solvents were purchased from Cambridge Isotope Laboratories, Inc., degassed, and dried over activated 3-Å molecular sieves prior to use.

$[H(OEt_2)_2][BAr^F_4]$,[1] KC_8,[2] (TPB)Co(N_2),[3] (TPB)CoBr,[3] (SiP_3)Co(N_2),[4] $NArP_3$,[5] (PBP)Co(N_2),[6] CP_3H,[7] and $Co(PPh_3)_2I_2$[8] were prepared according to literature procedures. All other reagents were purchased from commercial vendors and used without further purification unless otherwise stated. Et_2O for NH_3 generation reactions was stirred over Na/K (≥ 2 hours) and filtered before use.

Physical Methods:

Elemental analyses were performed by Midwest Microlab, LLC (Indianapolis, IN). ^1H and ^{13}C chemical shifts are reported in ppm relative to tetramethylsilane, using ^1H and ^{13}C resonances from residual solvent as internal standards. ^{31}P chemical shifts are reported in ppm relative to 85% aqueous H_3PO_4. Solution phase magnetic measurements were performed by the method of Evans.[9] IR measurements were obtained as solutions or thin films formed by evaporation of solutions using a Bruker Alpha Platinum ATR spectrometer with OPUS software. Optical spectroscopy measurements were collected with a Cary 50 UV-vis spectrophotometer using a 1-cm two-window quartz cell. Electrochemical measurements were carried out in a glovebox under an N_2 atmosphere in a one compartment cell using a CH Instruments 600B electrochemical analyzer. A glassy carbon electrode was used as the working electrode and platinum wire was used as the auxiliary electrode. The reference electrode was $Ag/AgNO_3$ in THF. The ferrocene couple (Fc/Fc^+) was used as an internal reference. THF solutions of electrolyte (0.1 M tetra-*n*-butylammonium hexafluorophosphate, $TBAPF_6$) and analyte were also prepared under an inert atmosphere. X-band EPR spectra were obtained on a Bruker EMX spectrometer.

X-ray Crystallography:

X-ray diffraction studies were carried out at the Caltech Division of Chemistry and Chemical Engineering X-ray Crystallography Facility on a Bruker three-circle SMART diffractometer with a SMART 1K CCD detector. Data was collected at 100K using Mo Kα radiation ($\lambda = 0.71073$ Å). Structures were solved by direct or Patterson methods using SHELXS and refined against *F*2 on all data by full-matrix least squares with SHELXL-97. All non-hydrogen atoms were refined anisotropically. All hydrogen atoms were placed at geometrically calculated positions and refined using a riding model. The isotropic displacement parameters of all hydrogen atoms were fixed at 1.2 (1.5 for methyl groups) times the U_{eq} of the atoms to which they are bonded.

Notes specific to individual structures:

The 12-crown-4 fragments are disordered for $[Na(12\text{-crown-}4)_2][(TPB)Co(N_2)]$. One 12-crown-4 (with O atoms labeled O5-O8 and O50-O80) is fully disordered over two unique positions. The other 12-crown-4 (O atoms labeled O1-O4) shows a disorder in the methyl carbons but not the oxygen atoms. In all cases, the positions of the carbons could be located in the difference map and refined anisotropically and the hydrogen atoms were placed at geometrically calculated positions as usual. The oxygen atom in one of the solvent THF molecules (O10 and O100) is disordered over two positions. The other THF molecule (with O9) shows large thermal ellipsoids, potentially indicating an unresolved disorder of this moiety. A diethylether molecule was located on an inversion center and is therefore disordered about this symmetry element. The occupancies of all disordered fragments were freely refined and the bond lengths and angles were restrained to be the same for the disordered fragments. Hydrogen atoms were not included on any of the solvent molecules for these reasons.

The fluorine substituents on C143, C144, C152, and C168 in [(TPB)Co][BAr_4^F] are disordered by rotation about the C–C bonds to varying extents and were refined as two-part positional disorders in each case. The occupancies of the disordered fragments were freely refined and the bond lengths and angles were restrained to be the same for the disordered fragments.

One isopropyl group attached to P2 is disordered for (CP_3)Co(N_2); one methyl group (labeled C37A and C37B) is disordered over two positions. Each position was located in the difference map and refined anisotropically with hydrogen atoms calculated in the usual manner. The occupancies of the two fragments were refined freely. In addition, after refinement, the model displays large positive residual electron density located within 0.06 Å of CO1. This is likely due to unresolved disorder; attempts to include this as disorder with respect to the cobalt atom do not improve the model upon refinement. The residual electron density may also be due to poor data at high angles, as imposing a high-angle cutoff (using SHEL 100.0 0.84) during refinement reduces the residual density significantly. Importantly, the bond distances about CO1 do not change significantly when this restraint is imposed.

The isopropyl substituents on P3 are disordered for [(CP_3)Co(N_2)][BAr^F_4]. The disorder reflects simultaneous rotation of the methyl substituents about the methine carbon for each isopropyl group, which was modeled as a two-part positional disorder. All carbons in the disordered fragments were located in the difference map and refined anisotropically, with hydrogen atoms geometrically calculated in the usual manner. In addition, the CF_3 groups attached to C16B and C18B are disordered between two positions, reflecting rotation of the CF_3 group with simultaneous rotation of the arene fragment attached to B. Both CF_3 groups were refined as two-part positional disorders. In all cases, the occupancies of disordered fragments were freely refined and the bond lengths and angles were restrained to be the same for disordered fragments of the same type.

Computational Methods:

All computations were carried out using version 3.0.2 of the ORCA program system.[10] DFT calculations employed the BP86 exchange-correlation functional. The 6-31+G* basis set[11] was used for all geometry optimizations, while single point calculations were performed at the 6-311++G**[12] level of theory. The atomic coordinates of **2** and **5** obtained from XRD studies were used as inputs for geometry optimizations at the lower level of theory, and the optimized geometries obtained in this way were used as inputs for single point calculations of the electron densities at the higher level of theory. Molecular electrostatic potentials were computed from the calculated electron densities using the orca_vpot subroutine. Atomic charges were computed using the CHELPG method developed by Breneman and Wiberg.[13] Electrostatic potential maps were visualized using version 5 of the GaussView program.[14]

A1.2 Synthetic Details:

[Na(12-crown-4)$_2$][(TPB)Co(N$_2$)] (2):

To a -78 ˚C solution of (TPB)CoBr (70.5 mg, 0.0967 mmol) in THF (2 mL) was added a freshly prepared solution of $NaC_{10}H_8$ (23.5 mg $C_{10}H_8$, 0.222 mmol) in THF (3 mL). The solution was brought to RT and allowed to stir for six hours. Addition of 12-crown-4 (51.1 mg, 0.290 mmol) and removal of solvent *in vacuo* provided a dark red solid. Et_2O was added and subsequently removed *in vacuo*. The residue was suspended in C_6H_6 and filtered and the solids were washed with C_6H_6 (2 x 2 mL) and pentane (2 x 2 mL) to furnish a red solid (68.8 mg, 0.0660 mmol, 68%). Single crystals were grown by vapor diffusion of pentane onto a THF solution of the title compound that had been layered with Et_2O. ^1H NMR (400 MHz, THF-d_8) δ 7.41 (3H), 6.94 (3H), 6.66 (3H), 6.44 (3H), 3.64 (32H), 2.29 (br), 1.37 (6H), 1.20 (6H), 0.93 (6H), -0.26 (6H). ^{11}B NMR (128 MHz, THF-d_8) δ 9.32. ^{31}P NMR (162 MHz, THF-d_8) δ 62.03. IR (thin film, cm^{-1}): 1978 (N_2). Anal. Calcd. for $C_{52}H_{86}BCoN_2NaO_8P_3$: C, 59.32; H, 8.23; N, 2.66. Found: C, 59.05; H, 7.99; N, 2.47.

[(TPB)Co][BAr$^F_4$] (3):

To a -78 ˚C solution of (TPB)Co(N$_2$) (**1**) (91.5 mg, 0.135 mmol) in Et_2O (2 mL) was added solid [H(OEt$_2$)$_2$][BAr^F$_4$] (134.0 mg, 0.132 mmol). The reaction was brought to RT and vented to allow for the escape of H_2. The purple-brown solution was stirred for 1 hr. The solution was layered with pentane (5 mL) and stored at -35 ˚C to furnish red-purple single crystals of the title compound (162.9 mg, 0.0952 mmol, 82%) which were washed with pentane (3 x 2 mL). ^{1}H NMR (400 MHz, C_6D_6) δ 26.25, 23.80, 8.64, 8.44 ([BAr$^F_4$]), 7.88 ([BAr$^F_4$]), 6.33, -2.16, -3.68. UV-Vis (Et_2O, nm {L cm^{-1} mol^{-1}}): 585 {1500}, 760 {532}. Anal. Calcd. for $C_{68}H_{66}B_2CoF_{24}P_3$: C, 53.99; H, 4.40. Found: C, 53.94; H, 4.51.

(CP_3)Co(N_2) (5):

(CP_3)H (100 mg, 0.169 mmol) and $CoCl_2$ • 1.5 THF (40 mg, 0.169 mmol) were mixed at room temperature in THF (10 mL). This mixture was allowed to stir for one hour, yielding a homogeneous cyan solution. This solution was chilled to -78 ˚C, and a solution of MeMgCl in tetrahydrofuran (0.5 M, 0.560 mmol) was added in three 370 μL portions over three hours. The mixture was allowed to warm slowly to room temperature, and then was concentrated to *ca.* 1 mL. 1,4-dioxane (2 mL) was added, and the resultant suspension was stirred vigorously for at least 2 hours before filtration. The filtrate was concentrated to a tacky red-brown solid, which was extracted with 1:1 C_6H_6 : pentane (10 mL), filtered over celite and lyophilized to yield the product as a red powder (96 mg, 0.141 mmol, 83%). Crystals suitable for X-ray diffraction were grown via slow evaporation of a pentane solution. ^{1}H NMR (300 MHz, C_6D_6) δ 7.28 (br, 3H), 6.82 (m, 9H), 2.82 (oct., -C*H*, 3H), 2.09 (sept., -C*H*, 3H), 1.49 (m, 18H), 1.06 (dd, -CHCH_3, 9H), 0.30 (dd, -CHCH_3, 9H). ^{31}P{^{1}H} (121 MHz, C_6D_6): δ 47.39. IR (thin film, cm^{-1}): 2057 (N_2). Anal. Calcd. for $C_{37}H_{54}CoN_2P_3$: C, 65.48; H, 8.02; N, 4.13. Found: C, 64.14; H, 8.36; N, 4.03.

[(CP_3)Co(N_2)][BAr$^F_4$] (6):

5 (75 mg, 0.11 mmol) and $[Cp_2Fe][BAr^F_4]$ (122 mg, 0.12 mmol) were dissolved separately in diethyl ether (ca. 3 mL each) and the ethereal solutions were cooled to -78˚C. The chilled solution of $[Cp_2Fe][BAr^F_4]$ was added dropwise to the solution of **5**, and the resultant mixture was allowed to stir at low temperature for one hour. At this point, the mixture was allowed to warm to room temperature before filtration over celite and concentration to *ca.* 2 mL. The concentrated filtrate was layered with pentane, and placed in a freezer at -35˚C to induce crystallization. Decanting the mother liquor off crystalline solids and washing thoroughly with pentane yields $[(CP_3)Co(N_2)][BAr^F_4]$ (**6**) as dark green-brown crystals (147 mg, 0.095 mmol, 86%). Crystals suitable for X-ray diffraction were grown by slow diffusion of pentane vapors into an ethereal solution of **6** at -35˚C. μ_{eff} (5:1 d_8-toluene:d_8-THF, Evans' method, 23 °C): 3.49 μ_B. ^1H NMR (300 MHz, C_6D_6) δ 17.22, 9.94, 8.24 ($[BAr^F_4]$), 7.72 ($[BAr^F_4]$), 3.13, 2.57, 1.5 – -2 (br, m), –3.68. IR (cm^{-1}): 2182 (N_2, thin film), 2180 (N_2, solution). Elemental analysis shows low values for N consistent with a labile N_2 ligand, Anal. Calcd. for $C_{69}H_{66}BCoF_{24}N_2P_3$: C, 53.75; H, 4.31; N, 1.82. Found: C, 53.86; H, 4.31; N, 0.27. Note: The magnetic moment for **6** in solution may be complicated by some degree of solvent exchange for N_2 at the cobalt center. Freeze-pump-thaw experiments monitored by optical spectroscopy establish that the N_2 ligand is labile in solution (see Figure A1.6). Low temperature (80 K) EPR spectroscopy in a solvent of lower donicity (2-Me-THF) is consistent with a low spin, S = 1/2 species (see Figure A1.7).

$[(NArP_3)CoCl][BPh_4]$:

THF (5 mL) was added to a solid mixture of $NArP_3$ (58 mg, 91.2 mmol), $CoCl_2$ (12 mg, 92.4 mmol) and $NaBPh_4$ (31 mg, 90.6 mmol). The reaction was stirred for 4 hours at room temperature during which the color evolved from yellow to green to purple. The solvent was removed *in vacuo* and the residue was taken up in dichloromethane. The suspension was filtered over a plug of Celite and the filtrate was dried yielding a purple powder (86 mg, 82.1 mmol, 90%). Single crystals were grown by slow evaporation of a saturated solution of $[(NArP_3)CoCl][BPh_4]$ in diethyl ether/dichloromethane (1:2 v:v). ^1H NMR (CD_2Cl_2, 300 MHz) δ 177.77, 37.50, 23.78, 13.48, 12.96, 7.37, 7.08, 6.92, 4.41, 1.50, -3.60, -9.81; UV-Vis (THF, nm {L cm^{-1} mol^{-1}}): 564 {452}, 760 {532}; μ_{eff} (CD_2Cl_2, Evans' method, 23 °C): 3.97 μ_B. Anal. Calcd. for $C_{63}H_{80}BClCoNP_3$: C, 72.10; H, 7.68; N, 1.33. Found: C, 71.97; H, 7.76; N, 1.30.

Treatment of $[(TPB)Co(N_2)][Na(12\text{-crown-}4)_2]$ (2) with 10 equiv $[H{\bullet}(OEt_2)_2][BAr^F_4]$ and 12 equiv KC_8:

$[(TPB)Co(N_2)][Na(12\text{-crown-}4)_2]$ (10 mg, 0.01 mmol) was suspended in Et_2O (0.5 mL) in a 20 mL scintillation vial equipped with a stir bar. This suspension was cooled to −78 °C in a cold well inside of a N_2 glovebox. A solution of $[H{\cdot}(OEt_2)_2][BAr^F_4]$ (95 mg, 0.094 mmol) in Et_2O (1.5 mL) similarly cooled to −78 °C was added to this suspension in one portion with stirring. Residual acid was dissolved in cold Et_2O (0.25 mL) and added subsequently. This mixture was allowed to stir for 5 minutes. Then KC_8 (16 mg, 0.119 mmol) was suspended in cold Et_2O (0.75 mL) and added to the reaction mixture over the course of 1 minute. The vial was then sealed, and the reaction was allowed to stir for 40 min at −78 °C before being warmed to room temperature and stirred for 15 min. The reaction mixture was then filtered and evaporated to dryness under vacuum. The resulting residue was extracted with C_6D_6 and submitted to ^{31}P NMR spectroscopy, revealing a signal consistent with uncoordinated phosphine at 10.8 ppm (Figure A1.1).

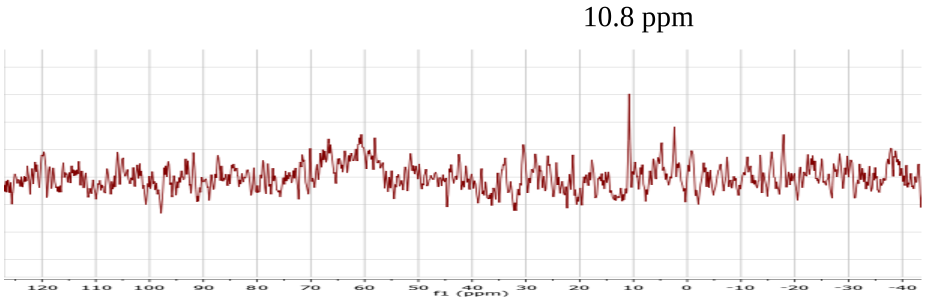

Figure A1.1: ^{31}P NMR of reaction mixture

A1.3 Ammonia Quantification:

A Schlenk tube was charged with HCl (3 mL of a 2.0 M solution in Et_2O, 6 mmol). Reaction mixtures were vacuum transferred into this collection flask. Residual solid in the reaction vessel was treated with a solution of [Na][O-*t*-Bu] (40 mg, 0.4 mmol) in 1,2-dimethoxyethane (1 mL) and sealed. The resulting suspension was allowed to stir for 10 min before all volatiles were again vacuum transferred into the collection flask. After completion of the vacuum transfer, the flask was sealed and warmed to room temperature. Solvent was removed in vacuo, and the remaining residue was dissolved in H_2O (1 mL). An aliquot of this solution (20 μL) was then analyzed for the presence of

NH_3 (present as $[NH_4][Cl]$) by the indophenol method.[15] Quantification was performed with UV−vis spectroscopy by analyzing absorbance at 635 nm.

Standard NH_3 Generation Reaction Procedure with $[(TPB)Co(N_2)][Na(12\text{-crown-}4)_2]$ (2):

$[(TPB)Co(N_2)][Na(12\text{-crown-}4)_2]$ (2.2 mg, 0.002 mmol) was suspended in Et_2O (0.5 mL) in a 20 mL scintillation vial equipped with a stir bar. This suspension was cooled to −78 °C in a cold well inside of a N_2 glovebox. A solution of $[H\cdot(OEt_2)_2][BAr^F_4]$ (95 mg, 0.094 mmol) in Et_2O (1.5 mL) similarly cooled to −78 °C was added to this suspension in one portion with stirring. Residual acid was dissolved in cold Et_2O (0.25 mL) and added subsequently. This mixture was allowed to stir 5 minutes at −78 °C, before being transferred to a precooled Schlenk tube equipped with a stir bar. The original reaction vial was washed with cold Et_2O (0.25 mL) which was added subsequently to the Schlenk tube. KC_8 (16 mg, 0.119 mmol) was suspended in cold Et_2O (0.75 mL) and added to the reaction mixture over the course of 1 minute. The Schlenk tube was then sealed, and the reaction was allowed to stir for 40 min at −78 °C before being warmed to room temperature and stirred for 15 min.

Table A1.1: UV-vis quantification results for standard NH_3 generation experiments with $[(TPB)Co(N_2)][Na(12\text{-crown-}4)_2]$ (**2**)

Iteration	Absorbance (635 nm)	Eq. NH_3/Co	% Yield Based on H^+

A	0.225	2.3	16
B	0.187	2.1	14
C	0.199	2.2	14
D	0.240	2.5	18
E	0.255	2.8	19
F	0.197	2.2	14
Average	0.217 ± 0.027	2.4 ± 0.3	16 ± 2

Hydrazine was not detected in the catalytic runs using a standard UV-Vis quantification method.[16]

Standard NH_3 Generation Reaction Procedure with (TPB)Co(N_2) (1):

The procedure was identical to that of the standard NH_3 generation reaction protocol with the changes noted. The precursor used was (TPB)Co(N_2) (1.3 mg, 0.002 mmol).

Table A1.2: UV-vis quantification results for standard NH_3 generation experiments with (TPB)Co(N_2) (**1**)

Iteration	Absorbance (635 nm)	Eq. NH_3/Co	% Yield Based on H^+
A	0.064	0.7	4
B	0.058	0.6	4
C	0.107	1.2	8
Average	0.076 ± 0.027	0.8 ± 0.3	5 ± 2

Standard NH_3 Generation Reaction Procedure with $[(TPB)Co][BAr^F_4]$ (3):

The procedure was identical to that of the standard NH_3 generation reaction protocol with the changes noted. The precursor used was $[(TPB)Co(N_2)][BAr^F_4]$ (2.3 mg, 0.002 mmol).

Table A1.3: UV-vis quantification results for standard NH_3 generation experiments with $[(TPB)Co][BAr^F_4]$ (**3**)

Iteration	Absorbance (635 nm)	Eq. NH_3/Co	% Yield Based on H^+
A	0.092	1.4	6
B	0.122	1.8	9
C[1]	0.091	1.5	6
Average	0.107 ± 0.021	1.6 ± 0.2	7 ± 1

[1] Used 2.0 mg (0.001 mmol) of catalyst; omitted from average absorbance

Standard NH_3 Generation Reaction Procedure with (TPB)CoBr:

The procedure was identical to that of the standard NH_3 generation reaction protocol with the changes noted. The precursor used was (TPB)CoBr (1.6 mg, 0.002 mmol).

Table A1.4: UV-vis quantification results for standard NH_3 generation experiments with (TPB)CoBr

Iteration	Absorbance (635 nm)	Eq. NH_3/Co	% Yield Based on H^+

A	0.035	0.3	2
B	0.101	1.0	7
C[1]	0.088	0.7	6
Average	0.068 ± 0.047	0.7 ± 0.4	5 ± 3

[1] Used 2.0 mg (0.003 mmol) of catalyst; omitted from average absorbance

Standard NH_3 Generation Reaction Procedure with $(SiP_3)Co(N_2)$ (4):

The procedure was identical to that of the standard NH_3 generation reaction protocol with the changes noted. The precursor used was $(SiP_3)Co(N_2)$ (1.5 mg, 0.002 mmol).

Table A1.5: UV-vis quantification results for standard NH_3 generation experiments with $(SiP_3)Co(N_2)$

Iteration	Absorbance (635 nm)	Eq. NH_3/Co	% Yield Based on H^+
A	< 0.005	< 0.1	—

B	< 0.005	< 0.1	—
C	< 0.005	< 0.1	—
Average	—	< 0.1	—

Standard NH_3 Generation Reaction Procedure with $(CP_3)Co(N_2)$ (5):

The procedure was identical to that of the standard NH_3 generation reaction protocol with the changes noted. The precursor used was $(CP_3)Co(N_2)$ (1.4 mg, 0.002 mmol).

Table A1.6: UV-vis quantification results for standard NH_3 generation experiments with $(CP_3)Co(N_2)$

Iteration	Absorbance (635 nm)	Eq. NH_3/Co	% Yield Based on H^+
A	0.044	0.21	1.5
B	< 0.005	< 0.1	—
C	< 0.005	< 0.1	—
Average	0.02 ± 0.02	0.1 ± 0.1	—

Standard NH_3 Generation Reaction Procedure with $[(NArP_3)CoCl][BPh_4]$:

The procedure was identical to that of the standard NH_3 generation reaction protocol with the changes noted. The precursor used was $[(NArP_3)CoCl][BPh_4]$ (1.9 mg, 0.002 mmol).

Table A1.7: UV-vis quantification results for standard NH_3 generation experiments with $[(NArP_3)CoCl][BPh_4]$

Iteration	Absorbance (635 nm)	Eq. NH_3/Co	% Yield Based on H^+
A	< 0.005	< 0.1	—
B	< 0.005	< 0.1	—
C	< 0.005	< 0.1	—
Average	—	< 0.1	—

Standard NH_3 Generation Reaction Procedure with (PBP)Co(N_2):

The procedure was identical to that of the standard NH_3 generation reaction protocol with the changes noted. The precursor used was (PBP)Co(N_2) (1.1 mg, 0.002 mmol).

Table A1.8: UV-vis quantification results for standard NH_3 generation experiments with (PBP)Co(N_2)

Iteration	Absorbance (635	Eq. NH_3/Co	% Yield Based on

	nm)		H^+
A	0.021	0.15	1
B	0.03	0.29	2
C	0.057	0.62	4
Average	0.036 ± 0.019	0.4 ± 0.2	2 ± 1

Standard NH_3 Generation Reaction Procedure with $Co(PPh_3)_2I_2$:

The procedure was identical to that of the standard NH_3 generation reaction protocol with the changes noted. The precursor used was $Co(PPh_3)_2I_2$ (1.8 mg, 0.002 mmol).

Table A1.9: UV-vis quantification results for standard NH_3 generation experiments with $Co(PPh_3)_2I_2$

Iteration	Absorbance (635 nm)	Eq. NH_3/Co	% Yield Based on H^+
A[1]	0.036	0.3	2
B	0.036	0.3	2
C	0.046	0.4	3
Average	0.041 ± 0.007	0.4 ± 0.1	2 ± 0.4

[1] Used 2.0 mg (0.0024 mmol) of catalyst; omitted from average absorbance

Standard NH_3 Generation Reaction Procedure with $CoCp_2$:

The procedure was identical to that of the standard NH_3 generation reaction protocol with the changes noted. The precursor used was $CoCp_2$ (0.6 mg, 0.003 mmol).

Table A1.10: UV-vis quantification results for standard NH_3 generation experiments with $CoCp_2$

Iteration	Absorbance (635 nm)	Eq. NH_3/Co	% Yield Based on H^+
A	0.020	0.09	1
B	0.008	0.02	0
C	0.033	0.20	2
Average	0.020 ± 0.013	0.1 ± 0.1	1 ± 1

Standard NH_3 Generation Reaction Procedure with $Co_2(CO)_8$:

The procedure was identical to that of the standard NH_3 generation reaction protocol with the changes noted. The precursor used was $Co_2(CO)_8$ (0.4 mg, 0.001 mmol, 0.002 mmol Co) sampled as a 100 µL aliquot of a stock solution (2.0 mg $Co_2(CO)_8$ in 0.5 mL Et_2O).

Table A1.11: UV-vis quantification results for standard NH_3 generation experiments with $Co_2(CO)_8$

Iteration	Absorbance (635 nm)	Eq. NH_3/Co	% Yield Based on H^+
A	< 0.005	< 0.1	—
B	< 0.005	< 0.1	—
C	< 0.005	< 0.1	—
Average	—	< 0.1	—

NH_3 Generation Reaction of $[(TPB)Co(N_2)][Na(12\text{-crown-}4)_2]$ (2) with Reductant Added First Followed by Acid:

N.B.: The following experiment was conducted to study the effect of the order of addition of reagents in the NH_3 generation reaction with **2**.

$[(TPB)Co(N_2)][Na(12\text{-crown-}4)_2]$ (2.2 mg, 0.002 mmol) was suspended in Et_2O (0.5 mL) in a 20 mL scintillation vial. This suspension was cooled to −78 °C in a cold well inside of a N_2 glovebox. This suspension was transferred to a precooled Schlenk tube equipped with a stir bar. Residual solid was suspended in additional cold Et_2O (2 x 0.25 mL) and transferred subsequently. To this mixture was added a precooled suspension of KC_8 (16 mg, 0.119 mmol) in 0.5 mL Et_2O. Residual solid was suspended in additional cold Et_2O (2 x 0.25 mL) and transferred subsequently. This mixture was allowed to stir for 5 minutes at −78 °C. To this mixture was then added a similarly cooled to −78 °C solution of $[H\cdot(OEt_2)_2][BAr^F_4]$ (95 mg, 0.094 mmol) in Et_2O (1.5 mL) in one portion with stirring. Residual acid was dissolved in cold Et_2O (0.25 mL) and added subsequently. The Schlenk tube was then sealed, and the reaction was allowed to stir for 40 min at −78 °C before being warmed to room temperature and stirred for 15 min.

Table A1.12: UV-vis quantification results for NH_3 generation experiments with $[(TPB)Co(N_2)][Na(12\text{-crown-4})_2]$ (**2**) and reductant being added first

Iteration	Absorbance (635 nm)	Eq. NH_3/Co	% Yield Based on H^+
A[1]	0.175	2.2	13
B	0.153	1.7	11
Average	—	1.9 ± 0.4	12 ± 1

[1] Used 1.9 mg (0.0018 mmol) of catalyst; omitted from average absorbance

Calibration Curves for NH_3 and N_2H_4 Quantification

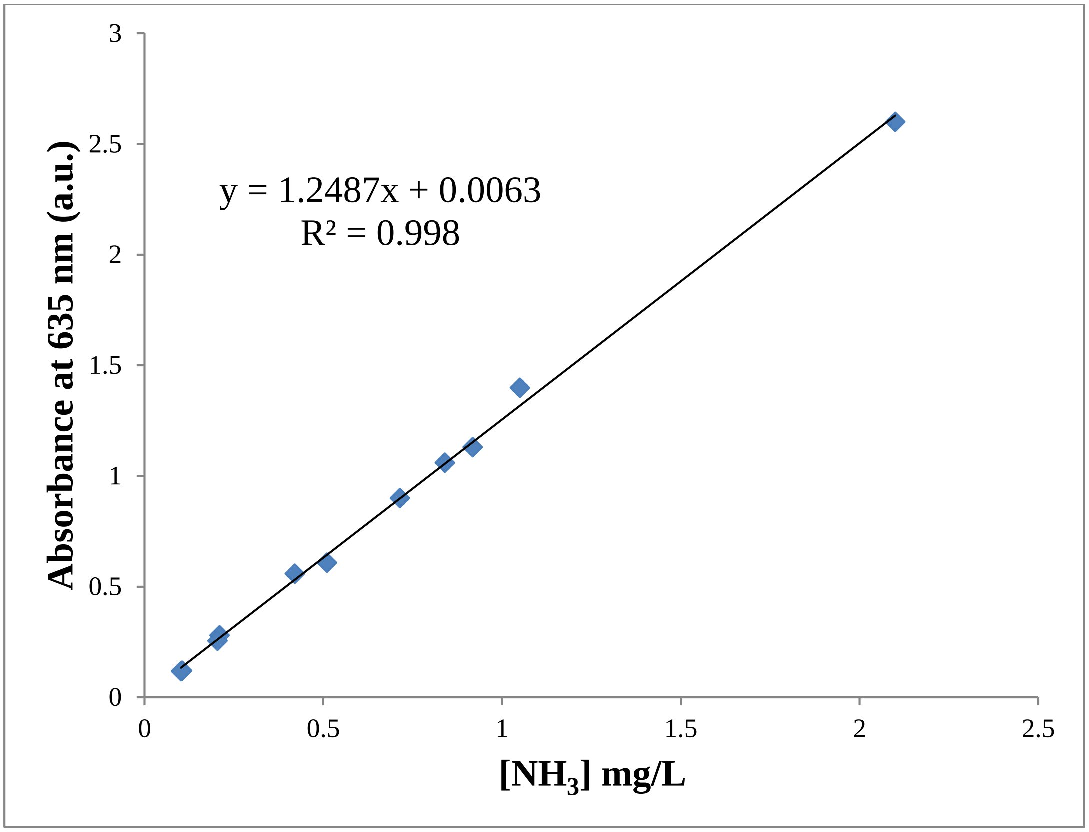

Figure A1.2: Calibration curve for NH_3 quantification by indophenol method.

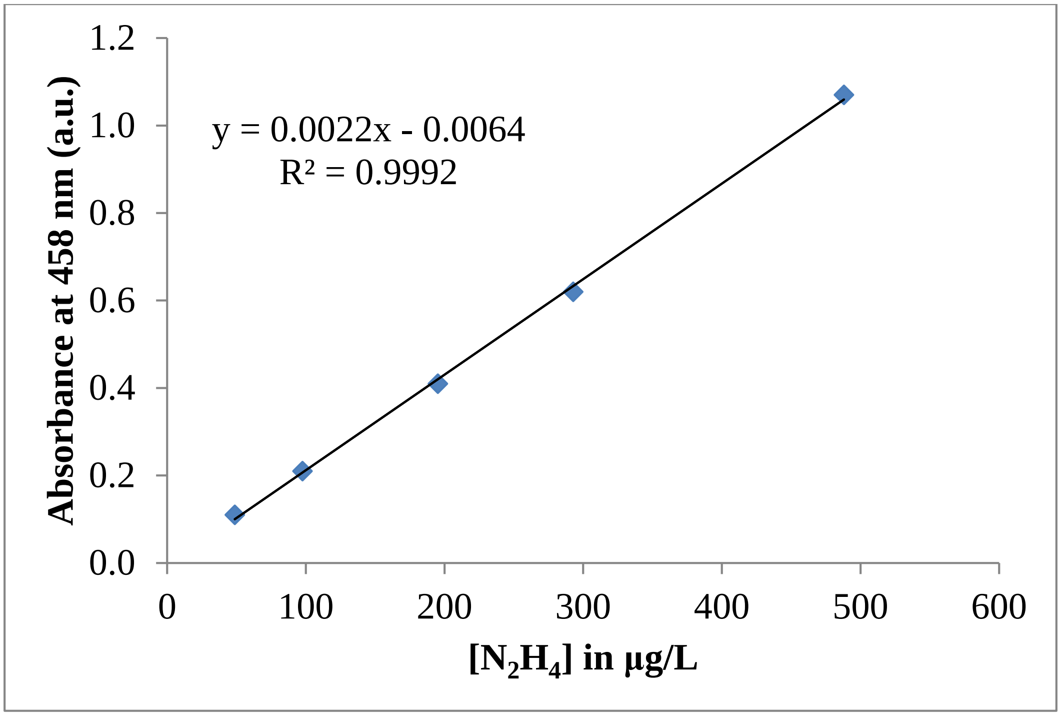

Figure A1.3: Calibration curve for UV-vis quantification of hydrazine.

A1.4 X-ray Diffraction Tables

Table A1.13: Crystal data and structure refinement for [Na(12-crown-4)$_2$][(TPB)Co(N$_2$)] (**2**) and [(TPB)Co][BAr$^F{}_4$] (**3**)

Identification code	**2**	**3**
Empirical formula	$C_{62}H_{86}BCoN_2NaO_{10.5}P_3$	$C_{68}H_{66}B_2CoF_{24}P_3$
Formula weight	1212.97	1512.67
Temperature/K	100(2)	100(2)
Crystal system	monoclinic	orthorhombic
Space group	$P2_1/n$	Pbca
a/Å	10.8142(5)	26.3920(15)
b/Å	27.5046(13)	19.7049(13)
c/Å	22.3660(10)	26.4995(19)
α/°	90	90
β/°	91.141(2)	90
γ/°	90	90

Volume/Å^3	6651.2(5)	13781.1(16)
Z	4	8
ρ_{calc}g/cm^3	1.211	1.458
μ/mm^{-1}	0.391	0.424
F(000)	2576	6176
Crystal size/mm^3	0.38 × 0.30 × 0.25	0.35 × 0.32 × 0.24
Radiation	MoKα (λ = 0.71073)	MoKα (λ = 0.71073)
2Θ range for data collection/°	3.94 to 86.26	3.72 to 64.06
Index ranges	$-20 \le h \le 20$, $-52 \le k \le 52$, $-43 \le l \le 43$	$-39 \le h \le 39$, $-23 \le k \le 29$, $-39 \le l \le 39$
Reflections collected	451328	377520
Independent reflections	49547 [R_{int} = 0.0632, R_{sigma} = 0.1797]	23962 [R_{int} = 0.0539, R_{sigma} = 0.0255]
Data/restraints/parameters	49547/1385/952	23962/1174/1007
Goodness-of-fit on F^2	1.091	1.052
Final R indexes [I>=2σ (I)]	R_1 = 0.0629, wR_2 = 0.1600	R_1 = 0.0459, wR_2 = 0.1084
Final R indexes [all data]	R_1 = 0.0999, wR_2 = 0.1797	R_1 = 0.0720, wR_2 = 0.1241
Largest diff. peak/hole / e Å^{-3}	1.78/-0.83	1.27/-1.34

Table A1.14: Crystal data and structure refinement for $(CP_3)Co(N_2)$ (**5**) and $[(CP_3)Co(N_2)][BAr^F{}_4]$ (**6**)

Identification code	**5**	**6**
Empirical formula	$C_{37}H_{54}CoN_2P_3$	$C_{50}H_{60}BN_2F_{24}P_3Co$
Formula weight	678.66	1541.89
Temperature/K	100(2)	100(2)
Crystal system	trigonal	orthorhombic
Space group	R-3	Pbca
a/Å	19.3720(4)	19.7869(17)
b/Å	19.3720(4)	25.670(2)
c/Å	48.1269(14)	26.680(3)
α/°	90	90
β/°	90	90
γ/°	120	90
Volume/Å^3	15641.1(8)	13552(2)
Z	18	8
ρ_{calc}g/cm^3	1.297	1.511
μ/mm^{-1}	0.660	0.421
F(000)	6516.0	6296.0
Crystal size/mm^3	0.380 × 0.330 × 0.210	0.5 × 0.3 × 0.2
Radiation	MoKα (λ = 0.71073)	MoKα (λ = 0.71073)
2Θ range for data	2.57 to 49.982°	3.014 to 69.836°

collection/°		
Index ranges	$-20 \le h \le 22$, $-23 \le k \le 23$, $-57 \le l \le 57$	$-31 \le h \le 30$, $-40 \le k \le 40$, $-42 \le l \le 22$
Reflections collected	56089	259812
Independent reflections	6124[R(int) = 0.0480]	28701[R(int) = 0.0932]
Data/restraints/parameters	6124/0/412	28701/138/1046
Goodness-of-fit on F^2	1.088	1.027
Final R indexes [I>=2σ (I)]	R_1 = 0.0738, wR_2 = 0.1910	R_1 = 0.0747, wR_2 = 0.1811
Final R indexes [all data]	R_1 = 0.0825, wR_2 = 0.2046	R_1 = 0.1609, wR_2 = 0.2254
Largest diff. peak/hole / e Å^{-3}	3.13/-0.82	1.42/-0.99

Table A1.15: Crystal data and structure refinement for [(NArP$_3$)CoCl][BPh$_4$]

Identification code	**[(NArP$_3$)CoCl][BPh$_4$]**
Empirical formula	C63H80BClCoNP3
Formula weight	1049.38
Temperature/K	100
Crystal system	triclinic
Space group	P-1
a/Å	10.9491(7)
b/Å	14.9096(10)
c/Å	17.8512(11)
α/°	83.935(3)
β/°	79.063(3)
γ/°	89.303(3)
Volume/Å^3	2845.1(3)
Z	2
ρ_{calc}g/cm^3	1.225
μ/mm^{-1}	0.472
F(000)	1118
Crystal size/mm^3	0.06 × 0.04 × 0.02
Radiation	MoKα (λ = 0.71073)
2Θ range for data	2.746 to 59.26

collection/°	
Index ranges	$-15 \le h \le 15$, $-20 \le k \le 20$, $-24 \le l \le 24$
Reflections collected	103727
Independent reflections	15990 [Rint = 0.0972, Rsigma = 0.0851]
Data/restraints/parameters	15990/0/646
Goodness-of-fit on F^2	1
Final R indexes [I>=2σ (I)]	R1 = 0.0457, wR2 = 0.0837
Final R indexes [all data]	R1 = 0.0986, wR2 = 0.0978
Largest diff. peak/hole / e Å^{-3}	0.53/-0.53

A1.5 DFT Calculations

Table A1.16: DFT Calculations

Optimized coordinates (Å) for $(CP_3)Co(N_2)$

Co	-6.493886	11.262439	3.205589
N	-6.498954	11.321632	1.436042
N	-6.509619	11.385450	0.291428
P	-8.326503	12.522417	3.530507
P	-4.468119	12.255409	3.466626
P	-6.717203	9.021548	3.482688
C	-6.448223	11.249419	5.315842
C	-7.421986	10.199514	5.854976
C	-6.831755	12.659131	5.809506
C	-3.940694	11.432267	5.038929
C	-7.788337	13.400564	5.064772
C	-5.023737	10.903746	5.778111
C	-7.568622	8.990937	5.132867
C	-7.603117	15.265630	6.637577
H	-7.887795	16.279035	6.939901
C	-4.742746	10.136998	6.931716
H	-5.568096	9.715601	7.513927
C	-8.127028	10.359559	7.068594
H	-8.021476	11.293607	7.630781
C	-2.350013	10.456601	6.623530
H	-1.315073	10.282269	6.938001
C	-3.418954	9.904690	7.345217
H	-3.227213	9.293903	8.234740
C	-8.171005	14.688130	5.486194
H	-8.895772	15.267989	4.902966
C	-6.290306	13.242663	6.974586
H	-5.546257	12.689483	7.558133
C	-6.663915	14.537630	7.381966
H	-6.211178	14.975618	8.278356
C	-2.618218	11.224609	5.475974
H	-1.778935	11.644663	4.910620
C	-8.973486	9.348391	7.556041
H	-9.520264	9.499953	8.493350
C	-9.117028	8.151983	6.838150
H	-9.780016	7.359107	7.201788
C	-8.410860	7.978161	5.633634
H	-8.543338	7.044435	5.079921
C	-8.870946	13.927902	2.377234
H	-9.579139	14.549161	2.960254
C	-7.900856	7.939713	2.420048
H	-8.881225	8.224247	2.846787
C	-2.974980	11.978914	2.306120

H	-2.138575	12.558042	2.749566
C	-11.073490	12.803315	4.510635
H	-11.460515	13.353930	3.634190
H	-10.701499	13.537242	5.246478
H	-11.933946	12.280737	4.970473
C	-3.155907	14.432185	4.936140
H	-2.159615	14.205199	4.513040
H	-3.263170	13.874622	5.878956
H	-3.168058	15.512103	5.177167
C	-4.285126	14.122349	3.935571
H	-5.248225	14.315181	4.440866
C	-9.996182	11.777970	4.114182
H	-9.674600	11.254092	5.032798
C	-5.136224	6.885483	4.794468
H	-5.782644	6.041163	4.502203
H	-5.478636	7.259548	5.772591
H	-4.112307	6.486414	4.928211
C	-5.111683	8.001046	3.732927
H	-4.436670	8.792666	4.106835
C	-4.174136	15.079503	2.733239
H	-4.366117	16.114986	3.072409
H	-4.893794	14.855473	1.930931
H	-3.157001	15.064980	2.302688
C	-9.609634	13.412697	1.125076
H	-9.843467	14.265270	0.459541
H	-10.561744	12.918383	1.372599
H	-8.989970	12.703071	0.551246
C	-10.558264	10.713993	3.153910
H	-11.275419	10.065197	3.690750
H	-9.756200	10.075649	2.751813
H	-11.095315	11.160582	2.300029
C	-7.678939	14.805649	1.967150
H	-6.977841	14.237435	1.333723
H	-7.125591	15.188887	2.840252
H	-8.036167	15.674064	1.381632
C	-4.537403	7.491093	2.393519
H	-3.454400	7.295446	2.497673
H	-4.667629	8.216410	1.571018
H	-5.011330	6.545616	2.083009
C	-7.792465	6.401362	2.524942

H	-8.705875	5.949101	2.092706
H	-7.694497	6.030410	3.555785
H	-6.938697	6.010390	1.948296
C	-7.904811	8.352731	0.936507
H	-6.920300	8.196505	0.460825
H	-8.178301	9.409648	0.801834
H	-8.640228	7.738209	0.384056
C	-3.216013	12.483650	0.865156
H	-3.500306	13.543308	0.807540
H	-4.003415	11.894901	0.368387
H	-2.285833	12.356421	0.279678
C	-2.570856	10.495897	2.228057
H	-3.389036	9.905335	1.785547
H	-2.324313	10.056729	3.207090
H	-1.685878	10.388535	1.571978

Total Energy: -3957.61934856 E_h

(BP86/6-311++G**)

Optimized coordinates (Å) for

$[(TPB)Co(N_2)]^-$

Co	5.278117	27.030827	17.095131
P	6.125307	28.046072	18.886124
P	3.060970	26.876003	16.921108
P	6.470673	27.144088	15.217970
N	5.627731	25.347668	17.547636
B	4.817109	29.224289	16.525303
C	5.694135	28.434162	14.141827
C	6.659431	29.741719	18.371700
C	8.356512	27.596015	15.041523
H	8.852351	26.898761	15.744263
C	2.349616	28.554979	17.254355
C	5.919014	30.203287	17.243942
C	4.249169	30.366935	14.143766
H	3.613935	31.089718	14.672539
C	3.298031	29.589854	17.025977
C	2.039333	26.364325	15.342342
H	2.508052	25.411985	15.027534
C	8.632318	29.033776	15.509744
H	9.724234	29.225133	15.517654
H	8.240887	29.232546	16.516177
H	8.165162	29.763658	14.825147
C	5.776139	28.504122	12.734994

H	6.347344	27.754542	12.173135
C	4.916069	29.360531	14.888824
C	7.654097	30.537197	18.977000
H	8.234583	30.154477	19.825542
C	7.696175	27.281935	19.678655
H	8.113875	28.047126	20.361713
C	6.505175	25.578416	14.108638
H	6.911463	25.889319	13.126608
C	5.097816	25.012789	13.875878
H	5.149571	24.119288	13.221278
H	4.435311	25.751866	13.395731
H	4.640644	24.714059	14.833576
C	8.769269	26.956916	18.629434
H	9.662297	26.521936	19.121695
H	9.088697	27.858071	18.080500
H	8.389141	26.224844	17.897330
C	5.086680	29.504431	12.026363
H	5.132996	29.537479	10.930024
C	6.213374	31.510860	16.783934
H	5.686654	31.896838	15.901416
C	7.428237	24.484391	14.686274
H	7.051899	24.114548	15.653220
H	8.463576	24.833229	14.841144
H	7.469612	23.621753	13.990762
C	8.994765	27.410878	13.648312
H	8.510202	28.063279	12.900483
H	8.967805	26.373773	13.274978
H	10.061346	27.711202	13.698303
C	2.863843	30.916667	17.272552
H	3.572857	31.743962	17.141225
C	7.207457	32.308686	17.379210
H	7.426705	33.305361	16.974755
C	5.200391	28.462003	20.552587
H	4.768821	27.487389	20.853188
C	4.046442	29.450732	20.325145
H	3.455086	29.562047	21.256355
H	3.367768	29.136369	19.521294
H	4.435636	30.447730	20.053591
N	5.856363	24.255842	17.849517
C	2.156451	25.748101	18.179342
H	1.079237	25.995091	18.113992
C	2.219078	27.389988	14.211139
H	1.747463	27.013325	13.281694
H	3.274732	27.607010	13.999641
H	1.735394	28.347886	14.470504

C	4.325635	30.444635	12.741090
H	3.772521	31.226887	12.204249
C	7.366421	26.022881	20.507880
H	6.952413	25.222948	19.873021
H	6.643132	26.219178	21.317461
H	8.291398	25.631095	20.977402
C	7.941743	31.818806	18.473149
H	8.737444	32.423937	18.925743
C	2.330158	24.252065	17.843386
H	3.384122	23.944599	17.933429
H	1.991543	23.999396	16.823928
H	1.738459	23.637376	18.550680
C	1.569705	31.207822	17.738468
H	1.280539	32.247270	17.943962
C	1.047615	28.839125	17.714406
H	0.337713	28.028272	17.918176
C	0.527783	26.123393	15.537653
H	0.020513	27.043374	15.878152
H	0.291949	25.313607	16.248614
H	0.074957	25.846405	14.563890
C	0.654345	30.165915	17.966300
H	-0.349915	30.380368	18.352394
C	2.613088	26.022466	19.619329
H	2.062411	25.370398	20.325778
H	2.433085	27.070631	19.910027
H	3.692725	25.819015	19.729581
C	6.065299	28.994192	21.714186
H	6.545033	29.952417	21.444344
H	6.851377	28.295209	22.046501
H	5.415134	29.194200	22.590266

Total Energy: -3944.45818385 E_h

(BP86/6-311++G**)

A1.6 Additional Characterization of Complexes

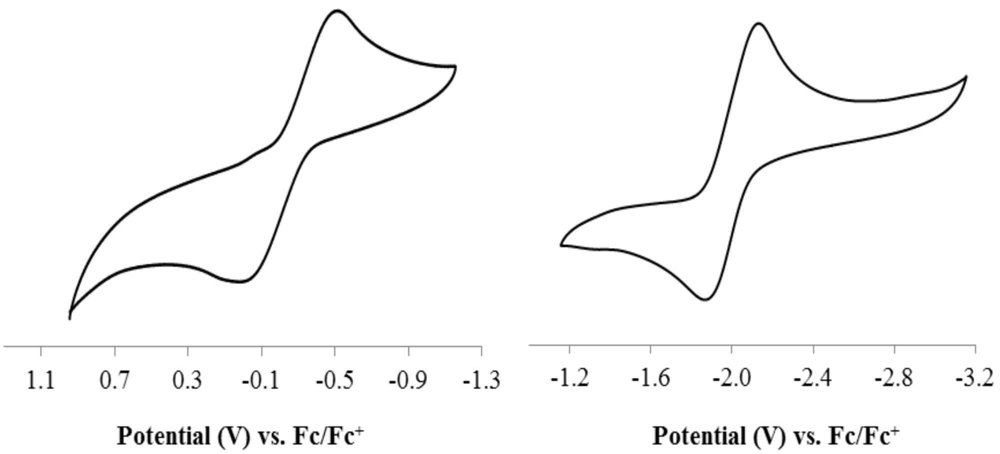

Figure A1.4: Cyclic voltammagram of (TPB)Co(N$_2$) (**1**) scanning oxidatively (left) and reductively (right) at 100 mV/sec in THF with 0.1 M TBAPF$_6$ electrolyte.

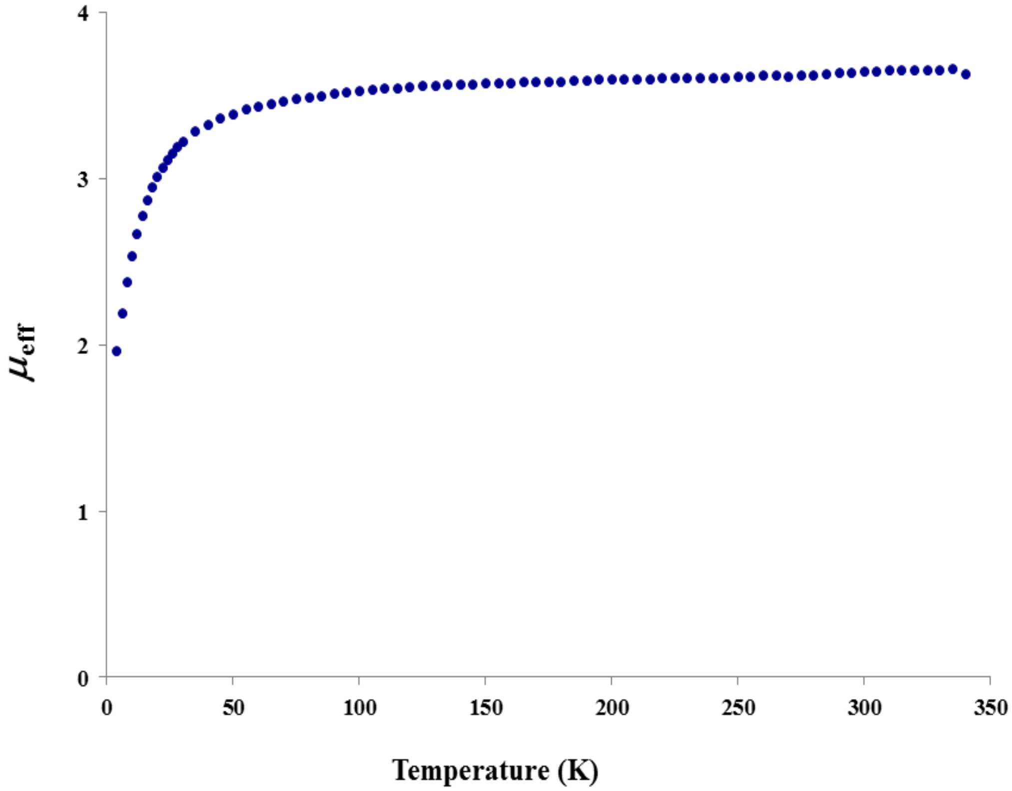

Figure A1.5: Temperature dependence of the magnetic susceptibility of [(TPB)Co][BAr$^F_4$] (**3**) as measured by SQUID magnetometry.

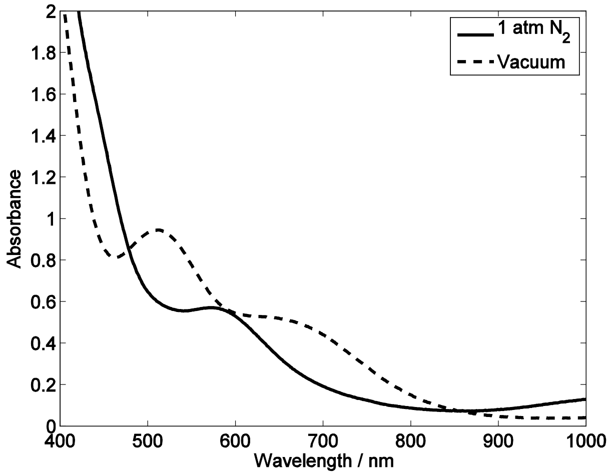

Figure A1.6: UV-Vis spectra of **6** under 1 atm N$_2$ and under static vacuum (after three freeze-pump-thaw cycles). Spectra collected of a 1 mM solution of **6** in THF at 298 K.

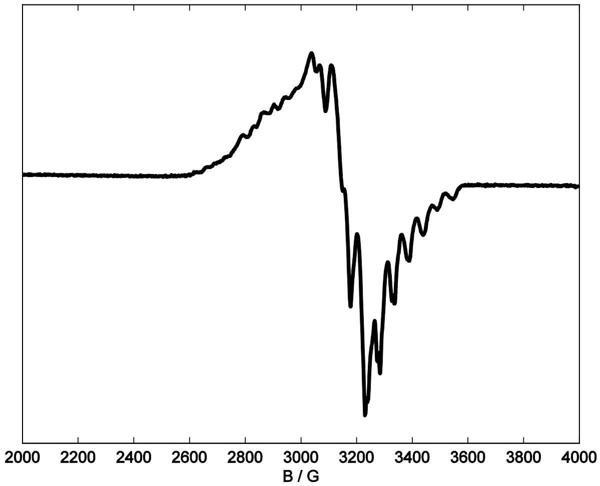

Figure A1.7: X-band EPR spectrum of **6** collected under 1 atm N$_2$ in 2-Me-THF at 80 K. No low-field features were detected.

A1.7 REFERENCES

1 Brookhart, M.; Grant, B.; Volpe Jr., A. F. *Organometallics* **1992**, *11*, 3920–3922.

2 Wietz, I. S.; Rabinovitz, M. J. *J. Chem. Soc., Perkin Trans.* **1993**, *1*, 117.

3 Suess, D. L. M.; Tsay, C.; Peters, J. C. *J. Am. Chem. Soc.* **2012**, *134*, 14158.

4 Whited, M. T.; Mankad, N. P.; Lee, Y.; Oblad, P. F.; Peters, J. C. *Inorg. Chem.* **2009**, *48*, 2507.

5 MacBeth, C. E.; Harkins, S. B.; Peters, J. C. *Can. J. Chem.* **2005**, *83*, 332.

6 Lin, T.-P.; Peters, J. C. *J. Am. Chem. Soc.* **2013**, *135*, 15310.

7 Creutz, S. E.; Peters, J. C. *J. Am. Chem. Soc.* **2014**, *136*, 1105.

8 Cotton, F. A.; Faut, O. D.; Goodgame, D. M. L.; Holm, R. H. *J. Am. Chem. Soc.* **1961**, *83*, 1780.

9 Evans, D. F. *J. Chem. Soc.* **1959**, 2003.

10 Nesse, F. *Comput. Mol. Sci.* **2012**, *2*, 73.

11(a) Hehre, W. J.; Ditchfield, R.; Pople, J. A. *J. Chem. Phys.* **1972**, *56*, 2257. (b) J. D.; Pople, J. A. *J. Chem. Phys.* **1975**, *62*, 2921. (c) Krishnan, R.; Binkley, J. S.; Seeger, R.; Pople, J. A. *J. Chem. Phys.* **1980**, *72*, 650. (d) McLean, A. D.; Chandler, G. S. *J. Chem. Phys.* **1980**, *72*, 5639. (e) Francl, M. M.; Pietro, W. J.; Hehre, W. J.; Binkley, J. S.; Gordon, M. S.; DeFrees, D. J.; Pople, J. A. *J. Chem. Phys.* **1982**, *77*, 3654. (f) Clark, T.; Chandrasekhar, J.; Schleyer, P. V. R. *J. Comp. Chem.* **1983**, *4*, 294. (g) Rassolov, V. A.; Pople, J. A.; Ratner, M. A.; Windus, T. L. *J. Chem. Phys.* **1998**, *109*, 1223.

12 Schaefer, A.; Horn, H.; Ahlrichs, R. *J. Chem. Phys.* **1992**, *97*, 2571.

13 Breneman, C. M.; Wiberg, K. B. *J. Comput. Chem.* **1990**, *11*, 361.

14 GaussView, Version 5, Dennington, Roy; Keith, Todd; Millam, John. Semichem Inc., Shawnee Mission, KS, 2009.

15 Weatherburn, M. W. *Anal. Chem.* **1967**, *39*, 971.

16 Watt, G. W.; Chrisp, J. D. *Anal. Chem.* **1952**, *24*, 2006.